Transition and Hot-Wire Measurements in Hypersonic Helium Flow

M. C. FISCHER* AND R. D. WAGNER*
NASA Langley Research Center, Hampton, Va.

Experiments have been performed to determine the influence of freestream disturbances on boundary-layer transition on sharp cones in a hypersonic wind tunnel. A constant current hot-wire anemometer was used to measure freestream and cone shock layer disturbances in two hypersonic helium tunnels. Comparison of these freestream and shock layer hot-wire measurements indicates that the disturbance level in percentage of local mean properties remains essentially unchanged by the cone shock. Transition Reynolds number was found to vary inversely with facility sound disturbance level and also to be strongly dependent on local Mach number.

Nomenclature

C = tunnel circumference, m
C_F = mean skin-friction coefficient
e = voltage fluctuation across hot wire, mV
M = Mach number
m = ρu, kg/m^2 sec
P = pressure, N/m^2
$\dot{q}$ = connective heat-transfer rate, W/m^2
R = Reynolds number
R/m = unit Reynolds number, per meter
R_{tunnel} = local radius from tunnel center line to wall, cm
$r_{\mathcal{L}}$ = radius from tunnel center line to model center line, cm
r_n = cone nose radius, cm
s = distance along cone surface from stagnation point, m
T = temperature, °K
u = streamwise velocity, m/sec
V = mean hot-wire voltage, mV
α = angle of attack, deg
Δe_m = mass flow sensitivity
Δe_t = total temperature sensitivity
δ = boundary-layer thickness, defined as $dP_{t,2}/dy = 0$, cm
δ^* = displacement thickness, cm
γ = ratio of specific heats
θ_c = cone half angle, deg

Subscripts
2 = behind normal shock
av = average value
c = cone shock layer
e = boundary-layer edge
t = stagnation conditions
tr = transition
w = wall conditions
∞ = freestream conditions

Superscripts
$\sim$ = root mean square
$(\bar{\ })$ = time average value
$()'$ = instantaneous value

Introduction

RESULTS from hypersonic boundary-layer transition investigations exhibit large disagreements when correlations are attempted. Continued transition studies for the sole purpose of obtaining absolute levels of transition Reynolds numbers constitute an exercise in futility. The early studies of Dryden,[1] Schubauer and Skramstad,[2] and others at low speeds verified that the tunnel disturbance level strongly influenced the location of boundary-layer transition. Apparently, the tunnel disturbance level dominates the high supersonic and moderately hypersonic transition results also, except that at these higher Mach numbers, sound (rather than the vorticity mode in low-speed tunnels) is the dominant disturbance mode in the free stream as shown by Wagner et al.[3] and Laufer.[4,5] Clearly, the documentation of a wind-tunnel transition investigation should include measurements of the freestream and shock-layer disturbance level. Hot-wire probes are presently the only proven means for obtaining such measurements in the freestream. However, no combined transition-hot-wire measurements exist above $M_e = 6.7$.

In the present study, the influence of tunnel disturbance level on cone boundary-layer transition was examined in two hypersonic helium tunnels. Combined measurements of surface transition location and freestream and shock-layer disturbance levels, detected with hot wires, were obtained at nominal freestream Mach numbers of 18 and 20 (edge Mach numbers from about 7.6 to 16.2). The tests were conducted in unheated flow, $T_w/T_{t,\infty} \approx 1.0$, and over a range of local Reynolds number based on model length from 9.4×10^6 to 87×10^6. The models consisted of three different half-angle cones.

Test Facilities

The experimental investigation was conducted in both the Langley 22-in. Hypersonic Helium Tunnel ($M_\infty \approx 20$) and in the 60-in. Mach 18 Leg of the Langley High Reynolds Number Helium Tunnel Complex. Each facility has a contoured axisymmetric nozzle and a freestream Mach number that varies slightly with freestream unit Reynolds number. Local cone unit Reynolds number varied from 19.8 to 57.0×10^6 per meter in the 22-in. facility and 27.8 to 48.9×10^6 per meter in the larger 60-in. facility. The tests were conducted in unheated flow ($T_{t,\infty} =$ 300°K) and with $T_w/T_{t,\infty} \approx 1.0$. Detailed descriptions of both the 22-in. and the 60-in. facilities are presented in Refs. 6 and 7, respectively.

Transition Models, Procedures, and Instrumentation

Three transition cone models were used in the present investigation, a 1.524-m (axial length) cone with $\theta_c = 2.87°$, a 0.61-m cone with $\theta_c = 5°$, and a 0.305-m, $\theta_c = 10°$ cone. Only the 1.524-m, $\theta_c = 2.87°$ cone was tested in both facilities. This cone was fabricated from 347 stainless steel and instrumented with 36-gage chromel-alumel thermocouples and stainless-steel pressure orifices. Skin thickness at the thermocouple location for the 2.87° cone was approximately 0.015 cm, and two nose radii tips of 0.0025 cm and 0.0102 cm were used. For the other two cones, $\theta_c = 5°$ and 10°, which were tested only in the 60-in. facility,

Presented as Paper 72–181 at the AIAA 10th Aerospace Sciences Meeting, San Diego, Calif., January 17–19, 1972; submitted January 24, 1972; revision received June 7, 1972.

Index categories: Boundary Layers and Convective Heat Transfer—Turbulent; Boundary-Layer Stability and Transition; Supersonic and Hypersonic Flow.

* Aerospace Engineer, Viscous Flow Section, Hypersonic Vehicle Division.

Table 1 Transition data obtained in the 22-in.-diam facility, $T_w/T_{t,\infty} \approx 1.0$

r_n, cm	$R_\infty/m \times 10^6$	$R_e/m \times 10^6$	s_{tr}, m	$R_{e,tr} \times 10^6$	M_∞	M_e	Distance of model axis off tunnel ℄, cm
0.0025	20.8	19.8	1.23	24.5	20.6	14.8	0.0
0.0025	26.5	24.3	1.08	26.3	21.0	15.4	0.0
0.0025	32.2	29.0	1.06	30.7	21.2	15.8	0.0
0.0025	35.6	32.2	1.06	34.0	21.3	15.9	0.0
0.0025	36.0	32.5	1.01	32.7	21.3	15.9	0.0
0.0025	42.8	38.2	0.878	33.6	21.4	16.2	0.0
0.0025	52.0	46.1	0.854	39.3	21.5	16.4	0.0
0.0025	53.6	47.5	0.803	38.1	21.6	16.5	0.0
0.0025	64.6	56.8	0.774	44.0	21.8	16.7	0.0
0.0102	32.5	29.4	1.03	30.6	21.2	15.8	0.0
0.0102	36.3	32.8	0.978	32.1	21.3	15.9	0.0
0.0102	42.8	38.2	0.904	34.5	21.4	16.2	0.0
0.0102	49.3	43.9	0.854	37.5	21.5	16.4	0.0
0.0102	54.5	48.3	0.775	37.5	21.6	16.5	0.0
0.0102	58.4	51.7	0.800	41.4	21.7	16.6	0.0
0.0102	65.0	57.0	0.757	43.1	21.8	16.7	0.0
0.0102	26.7[a]	24.4	1.02	24.8	21.0	15.4	0.0
0.0102	32.8[a]	29.7	1.03	30.6	21.1	15.7	+1.27
0.0102	33.0[a]	29.8	1.03	30.7	21.1	15.7	−1.27
0.0102	34.1[a]	30.8	0.889	27.4	21.1	15.7	0.0
0.0102	47.2[a]	42.2	0.864	36.4	21.5	16.3	0.0
0.0102	55.0[a]	48.6	0.686	33.4	21.6	16.5	0.0
0.0102	56.0[a]	49.4	0.775	38.7	21.6	16.5	−1.27
0.0102	56.0[a]	49.4	0.686	33.9	21.6	16.5	+2.54
0.0102	56.5[a]	49.9	0.724	36.1	21.6	16.5	+1.27
0.0102	57.1[a]	50.6	0.724	36.7	21.6	16.5	0.0

[a] Data obtained at later time with different test section installed.

30-gage chromel-alumel thermocouples were used and nominal wall thicknesses at the thermocouple stations were 0.104 cm and 0.0762 cm, respectively. Both the 5° and 10° half-angle cones had nose radii of about 0.0051 cm and were fabricated from Inconel 610.

Test Procedures and Instrumentation

Tests were conducted with the 2.87° half-angle cone in the 22-in. and 60-in. facilities and with the 5° and 10° half-angle cones in the 60-in. facility over a range of local unit Reynolds numbers of 19.8 to 57.0 × 10^6 per meter. A typical run time was about 5 sec; flow transients settled out per during the first 1 to $1\frac{1}{2}$ sec. Local heat-transfer rates on the cone surface were calculated as soon as flow conditions became constant. Initial model temperature was about 300°K, changing only about 5°K during a run. Conduction errors were found to be negligible. Boundary-layer edge conditions for the 2.87° half-angle cone in the 60-in. facility were determined from pitot surveys of the boundary-layer outer portion with a 0.102-cm-diam pitot probe. These surveys were conducted at one station, $s = 0.889$ m, and for two local unit Reynolds numbers $R_e/\text{m} = 27.9 \times 10^6$ and 43.7×10^6. Pitot pressures were measured with strain-gage diaphragm-type pressure transducers with an accuracy of ± 0.25%. Cone wall pressure was measured at the survey station using a diaphragm-type pressure transducer with a capacitive sensing circuit (accuracy of about ± 1%). Local edge Mach number was thus calculated from the pitot data by assuming the measured wall pressure to be constant across the boundary layer. Edge conditions on the 2.87° half-angle cone in the 22-in. facility were assumed to be the same as those calculated from pitot surveys of a cone of identical geometry previously tested in this facility[8] over a similar range of local conditions. Determination of the actual edge conditions for the 2.87° cone, with local Mach numbers from 13.2 to 16.2, was considered necessary because of viscous effects which lowered the edge Mach number considerably below the inviscid value. However, for the other two cones, $\theta_c = 5°$ and 10°, viscous effects on the edge conditions are less important and inviscid edge conditions were used.

Mass flow and total temperature fluctuation data were obtained in both the freestream and the cone shock layer (on the 2.87° and 10° cones and on the 16° cone used in Pt. I of Ref. 9) using a constant-current hot-wire anemometer. The techniques and instrumentation used are described in Ref. 3.

Additional tests were conducted to obtain spark schlierens of the 2.87° half-angle cone over a range of Reynolds numbers. In addition, the 2.87° half-angle model vibration during a run was measured with a vibration transducer mounted on the cone base. These measurements were made in both facilities to determine if excessive model deflections occurred, thus influencing the high Mach number transition results. For these tests only, the cone was tested at $\alpha = \frac{1}{3}°$ and $\frac{2}{3}°$ in addition to $\alpha = 0°$. The signal from the vibration transducer was input to a vibration meter, amplified, and then read out on an oscillograph. Frequency response capability of the complete system was about 500 Hz.

Stagnation pressures in the settling chamber were measured with strain gage diaphragm-type pressure transducers having an accuracy of about ± 0.25%. Stagnation temperatures were measured with bare iron-constantan thermocouples mounted in the settling chamber. All stagnation temperatures and pressures were corrected for real gas effects.[10] Freestream Reynolds numbers were corrected for low-temperature quantum effects on viscosity.[11]

Table 2 Transition data obtained in the 60-in.-diam facility $T_w/T_{t,\infty} \approx 1.0$

θ_c, deg	r_n, cm	$R_\infty/m \times 10^6$	$R_e/m \times 10^6$	s_{tr}, m	$R_{e,tr} \times 10^6$	M_∞	M_e
2.87	0.0102	27.3	27.8	1.12	31.1	17.8	13.2
2.87	0.0102	28.8	29.1	1.09	31.7	17.8	13.3
2.87	0.0102	29.2	30.3	1.04	31.6	17.8	13.3
2.87	0.0102	30.8	31.9	1.02	32.4	17.9	13.5
2.87	0.0102	34.8	34.6	0.965	33.4	18.0	13.7
2.87	0.0102	36.3	36.9	0.889	32.8	18.0	13.7
2.87	0.0102	40.1	40.1	0.825	33.2	18.1	13.9
2.87	0.0102	41.1	40.8	0.838	34.2	18.1	13.9
2.87	0.0102	44.0	43.8	0.788	34.5	18.2	14.1
2.87	0.0102	44.6	44.3	0.776	34.4	18.2	14.1
2.87	0.0102	45.1	43.7	0.812	35.5	18.3	14.2
2.87	0.0102	51.2	48.9	0.724	35.4	18.4	14.4
10.0	0.0051	37.7	30.9	0.249	7.7	18.1	7.6
10.0	0.0051	42.0	34.0	0.229	7.8	18.3	7.6
10.0	0.0051	46.7	37.3	0.203	7.6	18.4	7.6
10.0	0.0051	47.4	37.8	0.198	7.5	18.4	7.6
5.0	0.0051	37.5	40.0	0.528	21.2	18.2	12.0
5.0	0.0051	44.8	47.6	0.445	21.2	18.4	12.1

Results and Discussion

Transition Reynolds Numbers

Tables 1 and 2 list the pertinent parameters associated with the cone transition results in the 22-in. and 60-in. facilities, respectively. Cone boundary-layer transition at the model wall was determined from the experimentally measured heat-transfer distributions. Typical heat-transfer distributions for two unit Reynolds numbers in the 60-in. and 22-in. facilities are presented in Fig. 1. Since the tests were conducted in unheated flow, with $T_w/T_{t,\infty} \approx 1.0$, the heat flux was from the model to the flow

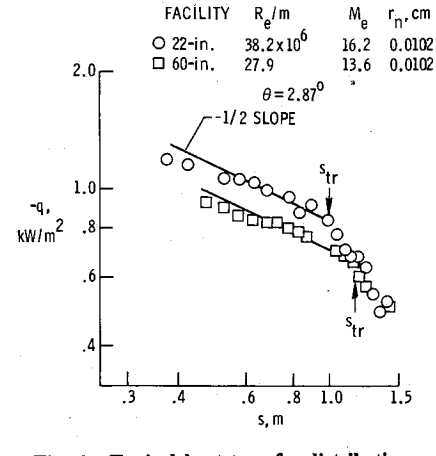

Fig. 1 Typical heat-transfer distributions.

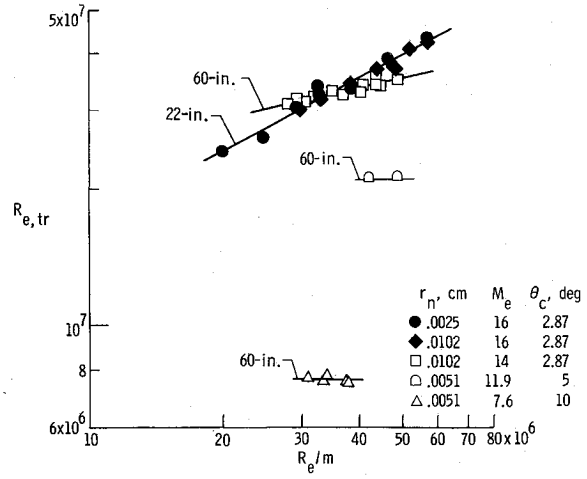

Fig. 2 Transition Reynolds number vs unit Reynolds number.

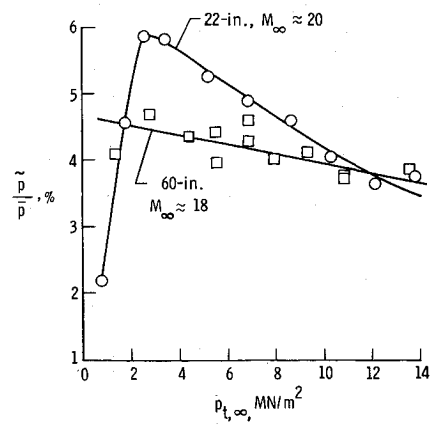

Fig. 3b Freestream and shock-layer hot-wire disturbance measurements: fluctuation level vs stagnation pressure.

$(-\dot{q})$. The location of transition at the wall was taken as the point where the heat-transfer data departed from the laminar $-\frac{1}{2}$ power slope. The pronounced decrease in the heat-transfer rate through the transition region is believed due to the variation of the recovery factor over this range. Transition data obtained with the 2.87° cone in both facilities exhibited a unit Reynolds number effect, but to different degrees (see Fig. 2).

The 2.87° cone transition data were obtained over a range of local Mach numbers because of the variation of freestream Mach number with unit Reynolds number. As observed in Fig. 2, there was no effect of a slight change in nose bluntness on the 2.87° cone transition data obtained in the 22-in. facility. Transition data obtained on the 5° and 10° half-angle cones in the 60-in. facility extended over a narrow unit Reynolds number range due to the short axial length of the model so that no trend with unit Reynolds number was perceivable.

Hot-Wire Fluctuation Measurements

A hot wire responds to instantaneous mass flow and total temperature fluctuations, and the rms and correlation of the mass flow and total temperature fluctuations can be obtained using the mode diagram approach as suggested by Kovasznay.[12] Mode diagrams consist of the virtual total temperature fluctuation $\tilde{e}/\Delta e_t V$ plotted vs the hot-wire sensitivity ratio $\Delta e_m/\Delta e_t$ (notation of Ref. 3). Typical mode diagrams from results in the 60-in. facility are presented in Fig. 3a for two stagnation pressures; two in the freestream, about 8.9 cm off the nozzle center line and another two in the cone shock layer of the 2.87° cone, about half way between the cone bow shock and the boundary-layer edge. Similar diagrams for measurements in the freestream of the 22-in. facility were presented in Ref. 3. First considering the freestream measurements, the linear mode diagrams indicate that the fluctuations in mass flow and total temperature in the freestream are generated by moving sound sources[3,5] located in the nozzle wall turbulent boundary layer.

The rms value of the mass flow fluctuations in percentage of local mean values is obtained from the slopes of the mode diagrams.[12] The freestream disturbance rms pressure fluctuation level for the 60-in. facility, which is directly related to the rms mass flow fluctuation level ($\tilde{p}/\bar{p} \approx \gamma \tilde{m}/\bar{m}$), is presented in Fig. 3b over a range of stagnation pressures, along with similar results[3] for the 22-in. facility. These measurements indicate that the disturbance level was nearly constant over the tunnel operating range of the larger Mach 18 facility; whereas, above 30×10^6 N/m^2 (boundary-layer transition on the 22-in. nozzle wall occurs at this pressure) the disturbance level decreased substantially with tunnel stagnation pressure in the 22-in. Mach 20 facility. One expects this result since the 60-in. tunnel wall boundary layer has a Reynolds number about five times greater than in the 22-in. tunnel owing to the slightly lower Mach number and the three times longer nozzle. Transition of the 60-in. nozzle wall boundary layer was not observed; the nozzle wall boundary layer is believed to be turbulent for all the test conditions.

In the shock layer specifically, the linear mode diagrams observed there as in the freestream (Fig. 3a) suggest that after passing through the shock the disturbance energy was not broken down into either of the other two modes, vorticity or entropy, since the presence of any two modes would be characterized by nonlinear mode diagrams.

Mode diagrams in the shock layers of the 10° and 16° cones were also linear (indicating predominantly sound present), and the rms mass flow fluctuations for all the cone shock-layer measurements are summarized in Fig. 3c. Therein, the ratios of local rms mass flow fluctuations (in percentage of the local

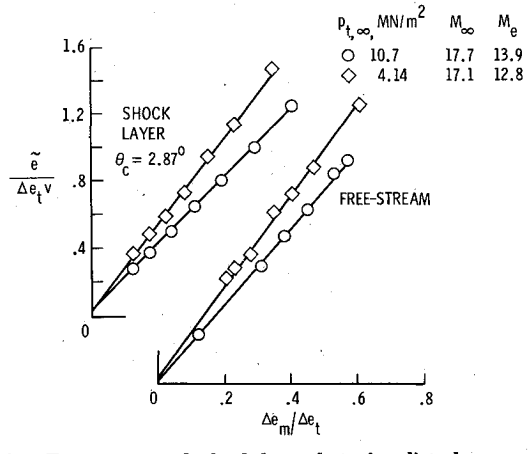

Fig. 3a Freestream and shock-layer hot-wire disturbance measurements: fluctuation mode diagrams.

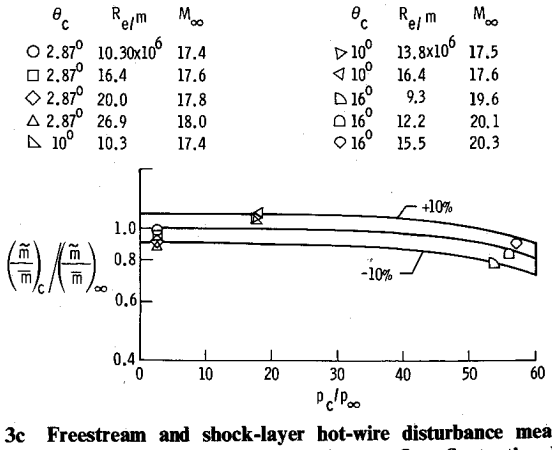

Fig. 3c Freestream and shock-layer hot-wire disturbance measurements: effect of shock strength on local mass flow fluctuation level.

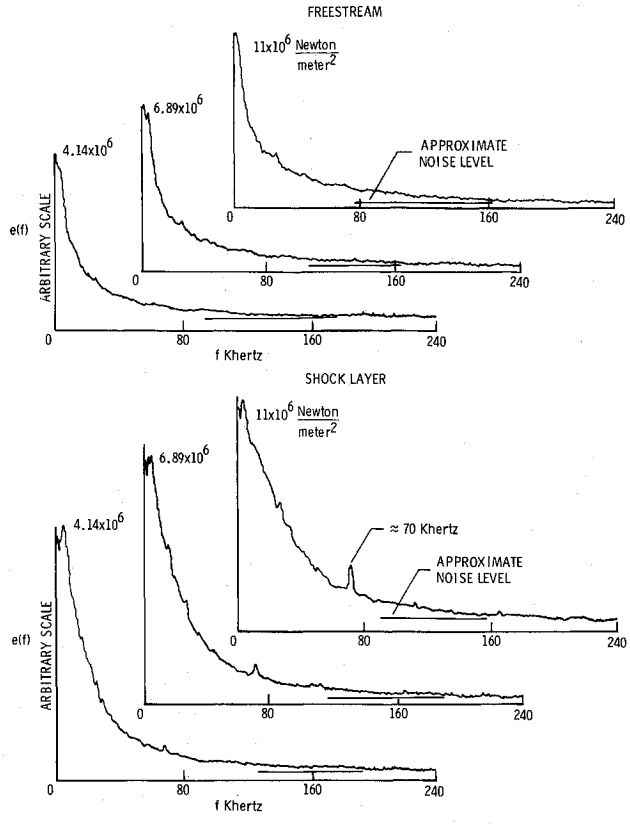

Fig. 3d Freestream and shock-layer hot-wire disturbance measurements: hot-wire spectra in the freestream and 2.87° cone shock-layer.

mean values) to the freestream values are shown for the different shock strengthe, P_c/P_∞, of the three cones. Note that at the high local Mach numbers of the present tests, and since the total temperature fluctuations are small, again $(\tilde{m}/\bar{m})_{local} \approx (p/\gamma p)_{local}$. Only for the somewhat stronger shocks on the 16° cones does there appear to be any significant change in the rms mass flow fluctuation in percent of local values. Note, however, that the actual sound pressure levels do increase about 10, 25, and 35 db for the 2.87°, 10°, and 16° cones, respectively. The rms total temperature fluctuations in percentage of total temperature $\tilde{T}_t/\bar{T}_t$ are given by the intercepts (at $\Delta e_m/\Delta e_t = 0$) of the mode diagrams. As indicated in Fig. 3a the $\tilde{T}_t/\bar{T}_t$ were always an order of magnitude smaller than the $\tilde{m}/\bar{m}$ and were difficult to obtain with accuracy. Nevertheless, a discernible increase in the $\tilde{T}_t/\bar{T}_t$ for the 16° cone was found; $\tilde{T}_t/\bar{T}_t$ increased from the stream value of about 0.06% to a postshock value of about 0.3%.

Spectra of the hot-wire signal in the freestream and the shock layer of the 2.87° cone are shown in Fig. 3d. (Spectra of the hot-wire signals in the other cone shock layers were not obtained.) The spectra in the freestream are typical of the wide-band turbulence as exists for sound radiated from a turbulent boundary layer. In the shock layer, some redistribution of the spectra seems to occur, especially at the highest stagnation pressure, but the more interesting feature is the gradual development of a discrete component, around 70 kHz in the spectra. This feature is believed to be associated with boundary-layer transition. Early in transition the schlieren photographs (to follow subsequently) show disturbances with scales on the order of twice the boundary-layer thickness. Assuming a disturbance velocity equal to the cone shock-layer velocity, the corresponding frequency would be about 70 kHz; the transition process on the cone appears to display some frequency selectivity.

The different unit Reynolds number effect on transition Reynolds number displayed by the 2.87° cone tested in the two facilities (Fig. 2) is consistent with the corresponding hot-wire measurements since the model transition processes are believed to be dominated by the disturbances radiated by the nozzle wall turbulent boundary layer. That is, the nearly flat disturbance level in the 60-in. facility (Fig. 3b) is consistent with the weak unit Reynolds number effect on the 60-in. 2.87° cone transition data (Fig. 2).

Because of the apparent insensitivity of transition Reynolds number to local Mach number for $M_e \geqq 13$, to be discussed subsequently, the 2.87° cone transition data were not corrected for the variation in local edge Mach number. The relationship between transition Reynolds number and the measured noise level for the 22-in. facility was $R_{e,tr} \propto (\tilde{P}/\bar{P}_\infty)^{-1.0}$ (Fig. 4) which indicates that (as previously found[3] at $M_e = 6.7$) the disturbance level has a strong influence on hypersonic transition. Transition results obtained in the 60-in. facility extended over a narrow range of $\tilde{P}/\bar{P}_\infty$, thus preventing a clear relationship between transition and noise to be established. However, the 2.87° cone results in this tunnel were consistent with the 22-in. tunnel results (see Fig. 4).

The effect of local hypersonic Mach number on transition was evaluated by comparing transition results obtained with the $\theta_c = 2.87°$, 5°, and 10° cones tested in the two facilities at the same freestream disturbance level. The data of Ref. 9 also are available to extend the comparison down to $M_e \approx 5$. The disturbance levels in the two tunnels were equal at approximately $P_{t,\infty} \approx 1170 \times 10^4$ N/m^2 (see Fig. 3b), which corresponded to $M_e = 7.6$, 11.9, and 14.1 ($\theta_c = 10°$, 5°, and 2.87°, respectively) in the 60-in. facility and $M_e = 5$ and 15.9 ($\theta_c = 16°$ and 2.87°, respectively), in the 22-in. facility. The transition results so obtained are presented in Fig. 5 over a wide Mach number range. The data display a strong effect of local Mach number in the low Mach region but also show a gradual reduction of the Mach number effect at the highest Mach numbers. For the 2.87° cone which was tested in both facilities, the transition Reynolds numbers at $M_e = 14.1$ (60-in. facility) and 15.9 (22-in. facility) were $R_{e,tr} = 34.5 \times 10^6$ and 32.7×10^6, respectively. The fact that these transition Reynolds numbers were nearly equal considering the corresponding local Mach number change is surprising, and in fact the tests of the 5° and 10° cones were conducted to define more clearly the influence of Mach number on wind-tunnel transition Reynolds number. If the sometimes-used relationship $R_{e,tr} \propto M_e^4$ existed, the transition Reynolds number for $M_e = 15.9$ would be more than 60% greater than for $M_e = 14.1$. Apparently, at high Mach number, boundary-layer transition Reynolds number becomes less dependent upon Mach number, at least for sound-dominated transition. Furthermore, it is believed that the scale of the turbulence radiating from the tunnel nozzle wall boundary layer incident upon the model has a minor role in the model boundary-layer transition process compared to the role of the level of the radiated pressure fluctuations. This conclusion is based on two observations. First, the inverse relationship which exists between transition Reynolds number and disturbance level presented in Fig. 4 from results in two facilities, different in physical size

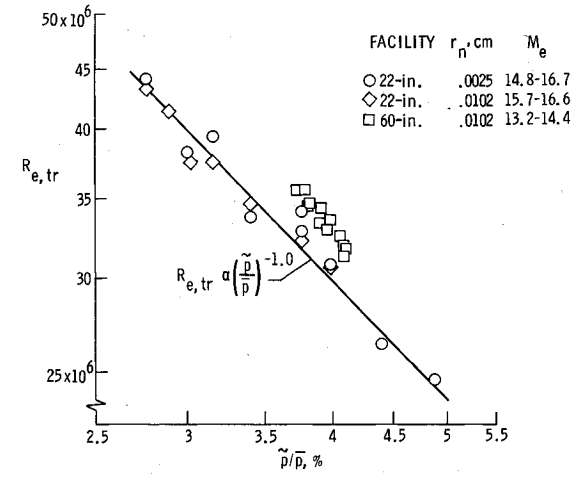

Fig. 4 Influence of tunnel disturbance level on hypersonic boundary-layer transition.

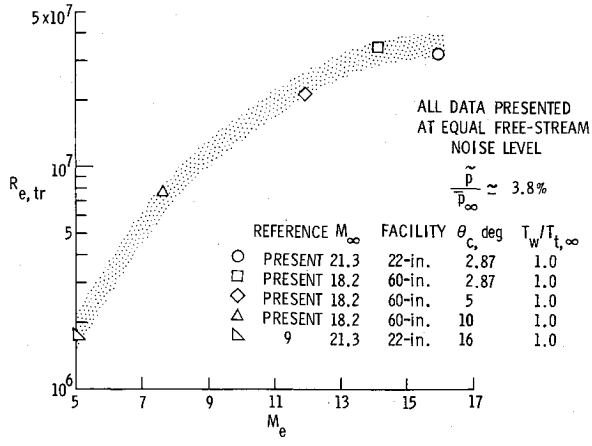

Fig. 5 Effect of local Mach number on cone transition Reynolds number.

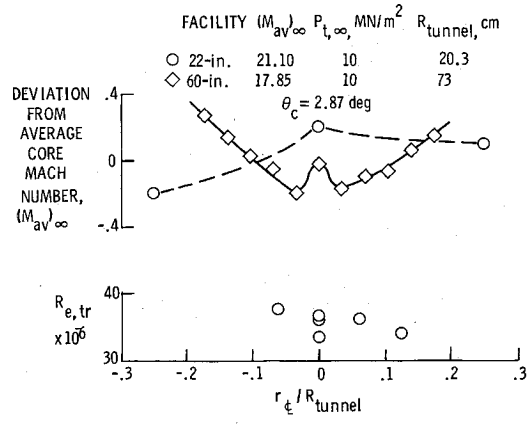

Fig. 7 Effect of off-centerline testing on transition Reynolds number in the 22-in. facility.

by a factor of 3, as well as the inverse relationship shown in Ref. 9 for cones tested in various facilities at $M_e = 5$, suggests a strong dependence on the disturbance level alone. Second, additional evidence that the scale of the incident radiation has little effect on transition can be found in Pate and Schueler's investigation.[13] In their study conducted at $M_e = 3$ and 5, transition and disturbance levels (measured on a model with a flush-mounted transducer) were measured under three different conditions of radiated incoming disturbance level; the model was shrouded, with and without a boundary-layer trip on the shroud, and the model was tested without a shroud. The scale of the incident disturbances certainly was different for each case, yet the transition Reynolds numbers were nearly equal whenever the measured disturbance levels were equal, apparently independent of the scale of the disturbances (see Figs. 5 and 6 of Ref. 13).

Additional tests were conducted in both facilities to determine if other parameters had influenced the 2.87° cone, high Mach number transition results, especially those results in the 22-in. facility which appeared to be low. Model vibration measured with a vibration pickup transducer mounted on the 2.87° cone base showed a peak-to-peak maximum base deflection of 2.54×10^{-4} cm in the 60-in. tunnel and half this amount in the 22-in. tunnel (Fig. 6). Corresponding vibration frequencies were about 10 Hz in the 22-in. facility and 18 Hz in the 60-in. facility. These deflections were believed to have an insignificant effect on the transition measurements, since the maximum cone tip fluctuating velocity ($u'_{+ip} \approx 10\ u'_{base}$) in percentage of local velocity was almost 2 orders of magnitude smaller than the velocity fluctuations in sound radiated from the tunnel walls ($u'_{+ip}/u_\infty \simeq 7 \times 10^{-5}\%$, $u'_{sound}/u_\infty \simeq 6 \times 10^{-3}\%$). Also, at these low frequencies, with a stream velocity of 1830 m/sec, the model vibrations would appear more as negligible quasi-steady angle-of-attack perturbations, $\alpha_{max} \approx 0.003°$.

Since both the hypersonic facilities used in this study have some Mach number variation across the test core (see Fig. 7), this Mach number gradient could have influenced the results. All transition data in both facilities were obtained with the cone axis aligned with the tunnel centerline. The 2.87° cone was therefore tested in the 22-in. $M_\infty \approx 20$ facility with the axis 1.27 cm and 2.54 cm above and 1.27 cm below the tunnel centerline. The effect of off-centerline testing on transition in the 22-in. facility was within the $\pm$ 10% measuring accuracy (Fig. 7). The results from the vibration and off-centerline tests tend to validate the transition results (Fig. 5) from tests with the model located on the tunnel centerline.

A comparison of the present 22-in. facility transition results with Pate's[14] cone noise-transition correlation is given in Fig. 8. Since the noise correlation of Ref. 14 was for the end of transition, and only the start of transition was measured in the present tests (the end of transition always occurred off the model), the present data were increased by a factor of 2.5, which should be appropriate for the end-of-transition location. However, the correlation prediction was about 60% higher than the data; or, expressed in another manner, the ratio of the end-to-start of transition for the experimental data must be about 4.3 to agree with the correlation, which seems unreasonably high. Values of mean turbulent skin friction for the nozzle wall

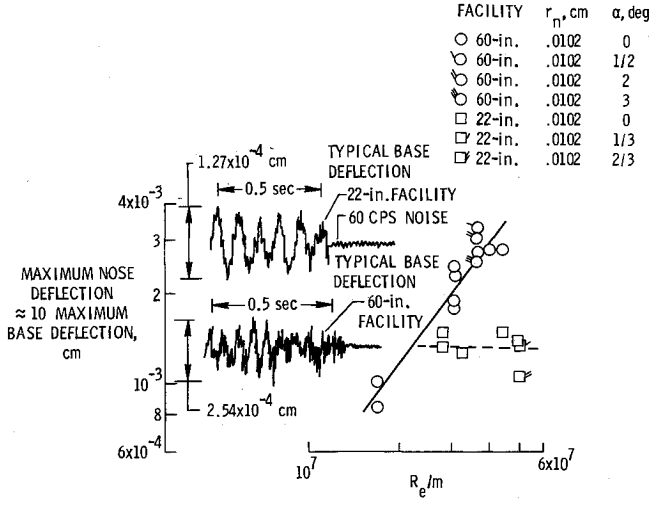

Fig. 6 Vibration of model during testing.

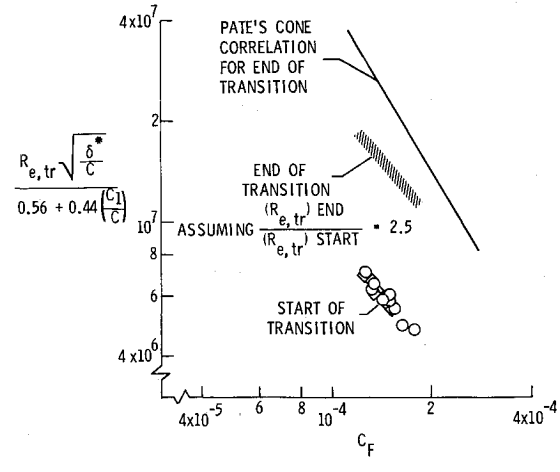

Fig. 8 Comparison of 22-in. 2.87° cone transition data with Pate's cone correlation.

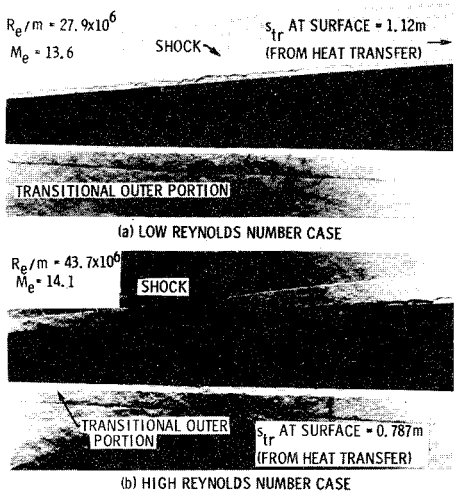

Fig. 9 Spark schlierens of the 2.87° cone in the 60-in. facility.

boundary layer used in the noise correlation were based on the Spalding-Chi[15] correlation modified for helium. Displacement thickness for the nozzle boundary layer were obtained from Ref. 16. The disagreement of the present transition data with Pate's noise-transition correlation stresses the need for a more precise means of relating disturbance level and transition Reynolds number, such as the present correlation, $R_{e,tr}$ vs P/P_∞, taken with the Mach number variation given in fig. 5.

Spark schlierens of the cone in the 60-in. facility revealed detailed boundary-layer structure. Typical schlierens at two Reynolds numbers are presented in Fig. 9 and indicate wavy structure at the boundary-layer edge with a scale of about twice the boundary-layer thickness. In each case, the wavy structure was evident far upstream of the wall transition location, as determined from heat-transfer data. The initial location of sizable boundary-layer disturbances at hypersonic speeds has experimentally been shown to occur in the outer portion of the boundary layer (critical layer region). This outer transitional growth ahead of the nominal wall transition location may be responsible for the observed disagreement between predicted and experimental thickness parameters upstream of transition.[17]

The present transition Reynolds number and disturbance level measurements are presented in Fig. 10 along with results from other investigations[2,9,18,19] (applicable only for laminar profiles with zero or negligible pressure gradients). Nearly the same inverse relation between the transition Reynolds number and the disturbance level was observed for results obtained in numerous air and helium facilities over a wide Mach number range. These results show that the sound radiated from the turbulent tunnel wall boundary layer dominates the transition,

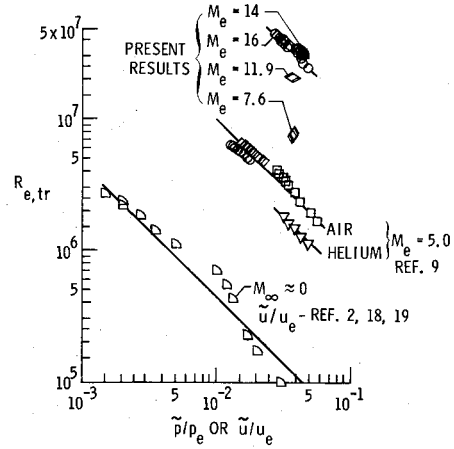

Fig. 10 Transition-disturbance level correlation summary.

and the transition Reynolds number varies inversely with the rms pressure level. There are, however, significant differences in the magnitude of the transition Reynolds number at the same rms pressure level. These differences suggest that the transition Reynolds number is also a function of local parameters governing the characteristics of the laminar profile—that is, local Mach number, total temperature, wall-to-total temperature ratio, and test gas.

Conclusions

Measurements of boundary-layer transition on 2.87°, 5°, and 10° half-angle cones were obtained in two hypersonic helium facilities at $T_w/T_{t,\infty} \approx 1.0$ in conjunction with hot-wire measurements of the freestream and shock-layer disturbance levels. The following conclusions can be made: 1) As observed at lower hypersonic Mach numbers, the tunnel disturbance level has a strong influence on cone boundary-layer transition up to at least $M_e = 16.7$. 2) Transition Reynolds number was found to vary inversely with facility sound disturbance level and also to be strongly dependent on local Mach number. 3) Hot-wire measurements in the freestream and cone shock layer indicate that the disturbance level in percent of local mean properties remains essentially unchanged by the cone shock.

References

[1] Dryden, H. L. and Kuethe, A. M., "Effect of Turbulence in Wind Tunnel Measurements," Rept 342, 1929, NACA.

[2] Schubauer, G. B. and Skramstad, H. K., "Laminar Boundary-Layer Oscillations and Transition on a Flat Plate," Rept 909, 1948, NACA.

[3] Wagner, R. D., Jr., Maddalon, D. V. and Weinstein, L. M., "Influence of Measured Free Stream Disturbance on Hypersonic Boundary-Layer Transition," *AIAA Journal*, Vol. 8, No. 9, Sept. 1970, pp. 1664–1670.

[4] Laufer, J., "Factors Affecting Transition Reynolds Numbers on Models in Supersonic Wind Tunnels." *Journal of the Aeronautical Sciences*, Vol. 21, July 1954, pp. 497–498.

[5] Laufer, J., "Aerodynamic Noise in Supersonic Wind Tunnels." Rept 20–378, 1959 Jet Propulsion Laboratory, Pasadena, Calif.; also *Journal of the Aeronautical Sciences*, Vol. 28, 1961, pp. 685–692.

[6] Arrington, J. P., Joiner, R. C., Jr. and Henderson, A., Jr., "Longitudinal Characteristics of Several Configurations at Hypersonic Mach Numbers in Conical and Contoured Nozzles," TN D-2498, 1964, NASA.

[7] Watson, R. D. and Bushnell, D. M., "Calibration of the Langley Mach 20 High Reynolds Number Helium Tunnel Including Diffuser Measurements," TM X–2353, Oct. 1971, NASA.

[8] Maddalon, D. V. and Henderson, A., Jr., "Boundary-Layer Transition on Sharp Cones at Hypersonic Mach Numbers," *AIAA Journal*, Vol. 6, No. 3, March 1968, pp. 424–431.

[9] Stainback, P. C., Fischer, M. C., and Wagner, R. D., "Effects of Wind-Tunnel Disturbances on Hypersonic Boundary-Layer Transition," AIAA Paper 72–181, San Diego, 1972.

[10] Erickson, W. D., "Real-Gas Correction Factors for Hypersonic Flow Parameters in Helium," TN D-462, Sept. 1960, NASA.

[11] Maddalon, D. V. and Jackson, W. E., "A Survey of the Transport Properties of Helium at High Mach Number Wind-Tunnel Conditions," TM X–2020, 1970, NASA.

[12] Kovasznay, L. S. G., "The Hot-Wire Anemometer in Supersonic Flow," *Journal of the Aeronautical Sciences*, Vol. 17, No. 9, Sept. 1950, pp. 565–572.

[13] Pate, S. R. and Schueler, C. J., "Radiated Aerodynamic Noise Effects on Boundary-Layer Transition in Supersonic and Hypersonic Wind-Tunnels," *AIAA Journal*, Vol. 7, No. 3, March 1969, pp. 450–457.

[14] Pate, S. R., "Measurement and Correlation of Transition Reynolds Number on Sharp Slender Cones at High Speeds," AEDC–TR–69, June 1969, Arnold Engineering Development Center, Tullahoma, Tenn.

[15] Spalding, D. B. and Chi, S. W., "The Drag of a Compressible Turbulent Boundary-Layer on a Smooth Flat Plate With and Without

Heat-Transfer," *Journal of Fluid Mechanics*, Vol. 18, P. I, Jan. 1964, pp. 117–143.

[16] Fischer, M. C., Maddalon, D. V., Weinstein, L. M. and Wagner, R. D., Jr., "Boundary-Layer Pitot and Hot-Wire Surveys at $M_\infty = 20$," *AIAA Journal*, Vol. 9, No. 5, May 1971, pp. 826–834.

[17] Fischer, M. C. and Maddalon, D. V., "Experimental Laminar, Transitional, and Turbulent Boundary-Layer Profiles on a Wedge at Local Mach Number 6.5 and Comparisons With Theory," TN D–6462, Sept. 1971, NASA.

[18] Dryden, H. L., "Air Flow in the Boundary-Layer Near a Plate," Rept. 562, 1936, NACA.

[19] Hall, A. and Hislop, G. S., "Experiments on the Transition of the Laminar Boundary-Layer on a Flat Plate," R. and M. 1843, 1938, British Aero Research Comm.

OCTOBER 1972 AIAA JOURNAL VOL. 10, NO. 10

Three-Dimensional Effects on Electron Density in a Blunt Body Laminar Boundary Layer

C. B. WATKINS* AND F. G. BLOTTNER†
Sandia Laboratories, Albuquerque, N. Mex.

Numerical solutions for the nonsimilar, laminar boundary layer on the most windward generator of a spherically blunted cone at angle of attack are described. Three-dimensional effects are properly treated by a quasi-two-dimensional symmetry-plane analysis. Electron number density distributions are calculated for chemically frozen boundary layers with catalytic walls at three angles of attack. Use of nonequilibrium boundary-layer edge conditions accounts for the swallowing of inviscid streamlines by the boundary layer. A comparison is made with axisymmetric equivalent cone numerical solutions and with a correlation used for axisymmetric boundary layers. The present results indicate a significant reduction in electron density at moderate angle of attack while equivalent cone solutions tend to predict electron number densities appreciably higher.

Nomenclature

c_i = mass fraction of species i, ρ_i/ρ
c_{p_i} = specific heat at constant pressure of species i, $\text{cm}^2/(\text{sec}^2 - {}^\circ\text{K})$
$\bar{c}_p$ = frozen specific heat at constant pressure of the mixture, $\sum_{i=1}^{NI} c_i c_{p_i}$, $\frac{\text{cm}^2}{(\text{sec}^2 - {}^\circ\text{K})}$
D_{ij} = binary diffusion coefficient, cm^2/sec
f' = nondimensional streamwise velocity ratio, u/u_e
g' = nondimensional crossflow velocity ratio, w/u_e
h_i = enthalpy of species i, cm^2/sec^2
k = thermal conductivity of the mixture, $g/(\text{sec } {}^\circ\text{K})$
Le_i = Lewis-Semenov number $\bar{c}_p \rho D_{ij}/k$
l = density-viscosity product, $\rho\mu/(\rho\mu)_r$
M = Mach number
M_i = molecular weight of species i, g/g-mole
N_e = electron number density, electrons/cm^3
NI = number of species
Pr = Prandtl number, $\bar{c}_p\mu/k$
p = pressure, $g/(\text{sec}^2\text{cm})$
R = perpendicular distance from axis along stagnation streamline, cm
R_N = nose radius, cm
R_s = perpendicular distance from stagnation streamline to point where streamline enters shock layer, cm
r = perpendicular distance from body axis, cm
$\mathcal{R}$ = universal gas constant, $\text{g-cm}^2/(\text{g-mole sec}^2\ {}^\circ\text{K})$
Sc_i = Schmidt number, Pr/Le_i
T = temperature, °K
U = total velocity along a streamline, cm/sec
u, v, w = velocity components in x, y, and φ directions, cm/sec
V = transformed normal velocity, see Eq. (3d)
V_∞ = freestream velocity, cm/sec
W_i = mass rate of formation of species i, $g/(\text{cm}^3 \text{ sec})$
x = distance along body, cm
y = distance along normal from surface, cm
α = angle of attack, deg
β = cone half-angle, deg
Δ = shock stand-off distance, cm
η = transformed normal coordinate, see Eq. (2b)
θ = nondimensional temperature ratio, T/T_e
μ = viscosity, g/(cm sec)
ρ = density, g/cm^3
φ = meridional angle, deg
ξ = transformed coordinate along body, see Eq. (2a)

Subscripts
b = body
e = conditions at outer edge of boundary layer
r = reference conditions
sh = shock
w = conditions at body surface or wall
∞ = freestream conditions
$()_{peak}$ = peak value for a given x/R_N

Received November 15, 1971; revision received April 6, 1972. The authors wish to express their thanks to D. E. Larson for his assistance in obtaining the numerical results of this paper. This work was supported by the U. S. Atomic Energy Commission.

Index categories: Boundary Layers and Convective Heat Transfer—Laminar; Reactive Flows.

* Staff Member, Numerical Fluid Dynamics Division; presently Assistant Professor, Department of Mechanical Engineering, Howard University, Washington, D.C. Member AIAA.

† Supervisor, Numerical Fluid Dynamics Division, Member AIAA.

Introduction

THE importance of three-dimensional effects in boundary-layer theory has long been recognized[1,2] and that class of problems dealing with the flow over bodies of revolution at angle of attack has great practical interest. Because of the complexities of these flows, most analyses make the problem tractable, either by resorting to approximate formulations, or by treating limiting cases where partial similarity reduces the number of independent variables. The approximate formulations include the negligible crossflow method,[3] small crossflow[4,5] and other perturbation techniques,[6] two-layer method,[7] and integral techniques.[8,9] Quasi-two-dimensional similar solutions have been obtained principally for the sharp cone.[10–14] Another noteworthy approach is the fully numerical solution.[15–18] Der[15] and Vvendenskaya[16] have obtained numerical solutions for three-dimensional boundary-layers on spherically blunted